MODELING THE DYNAMICS OF A REVERSE FLOW REACTOR

A Proposal for:

Dr. Antony Beris and Dr. Raul Lobo
CHEG 831/835
University of Delaware
Chemical & Biomolecular Engineering Department

By:

Pierre Desir
Jeff Horner
Josh Lansford

December 11th, 2015

Abstract

This work aims at modeling a reverse flow reactor (RFR) for the catalytic combustion of a lean methane feed at various inlet methane concentrations and superficial velocities. The purpose of this model is to analyze the dynamics of the RFR and determine the critical parameters that govern this process. This model was validated against a similar study conducted by Ordonez et al. at 3500 ppm methane with a 0.1 m/s superficial velocity (5 second residence time) [1]. These were the two most important parameters impacting the model and drove the time at which the flow had to be reversed. The RFR was modeled as a structured bed (monolithic) reactor and the operating conditions were set to those in the mentioned study. The partial differential mass and energy balance equations (PDEs) describing the reactor system were transformed into a large set of ordinary differential equations (ODEs) through discretization using the method of lines technique and evaluated in MATLAB using ode15s. To improve the computational efficiency of the model, several simplifications to the balance equations were made. Some of these simplifications included neglecting diffusive effects, neglecting the homogenous reaction, and neglecting the radial effects. This model consisted of four second order partial differential equations and will be referred to in the rest of this paper as the "full model". Run times for this model were very long, as will be discussed, so further simplifications were made to remove the wall energy balance and all diffusive effects resulting in 3 sets of first order partial differential equations. In the rest of this paper this model will be referred to as the "simplified model". The results obtained from both models were validated against those from literature at 3500 ppm methane and 0.1 m/s. The temperature and concentration profiles of this model matched those reported in literature at the same operating conditions. Both the model described here and the previous study show over 99% conversion of the methane within the critical switching time during the first run and with every subsequent flow reversal. In addition, the temperature profiles show that after several switches, the heat needed to drive the reaction is trapped in the center of the reactor. Although there are some slight differences in the temperatures obtained in this model and the model from literature, these are likely due to the discrepancies between the mass and heat transfer correlations used. An eigenvalue analysis was conducted on the solutions to the simplified model as well as the original model, and it was found that the solution is stable even at a low number of discretization points. Furthermore, the dynamics of the system were analyzed by determining the response of the model to small changes in the inlet concentration. It was found that the reactor could withstand sudden decreases in methane concentration and small increases in concentration. However large temporary increases in inlet methane concentrations would cause temperature to spike above the degradation point of the catalyst used. Nevertheless, if this is a significant concern in regarding temporary increases in temperature, another catalyst can be used.

Introduction

Greenhouse gases have been the focus of many environmental policies due to their negative effects on climate change. For the past couple of years, they have been shown to be one of the main active agents of global warming. Although these gases are generated in the environment from many different sources, they often result as byproducts of industrial processes. From that perspective, mining activities have played an important role in increasing the release of methane to the atmosphere. Studies have shown that mine air ventilation can contain up 1 vol% of methane [2]. Moreover, these emissions can be considered as a natural resource that can potentially be recovered as energy. Several methods have been proposed to efficiently use this methane through combustion and heat integration. The resulting CO2 is less of an environmental hazard since its global warming potential is 23 times lower than that of methane [1]. Although catalytic combustion of these methane streams has been proven to be one of the most efficient solutions, the low methane concentration remains a problem as the process becomes energetically expensive [1]. In order to remedy this problem, reverse flow catalytic reactors (RFRs) have been developed with the main functionality that these systems increase the conversion of hydrocarbons and the thermal efficiency of the process.

In reverse flow reactors, the directional flow of the feed is periodically reversed to use the heat released during combustion to further drive reaction of a fresh stream. These reactors are usually made of three sections for which the middle of the reactor is filled with catalyst and the ends are replaced with an inert material [1]. Initially, the reactor is pre-heated to the ignition temperature of the hydrocarbon present in the inlet stream, which in this case is 400 °C. The feed is at ambient temperature and low pressure to minimize energy requirements [1]. Heat is released and carried along the feed while the temperature increases throughout the reactor as combustion occurs. As the heat wave propagates throughout the reactor, the temperature decreases and before the reaction reaches extinction, the flow of the feed is reversed. This periodic flow reversal causes the heat release by combustion to be trapped in the mid-section of the reactor where catalyst is present. This heat is then used to increase the conversion of the reactants in the catalytic bed. The switching time, which is defined as the time interval between two consecutive flow reversals, becomes the parameter that needs to be optimized for a specific inlet feed concentration and superficial velocity. Likewise, it can be adjusted along with the gas velocity to accommodate different methane concentrations in the feed. It is best to make the switching time as long as possible without the heat escaping the reactor. As the switching time is lengthened the methane left over in the reactor when the flow is reversed becomes less and less significant. Furthermore, longer switching times give better stability and reduce the mechanical wear and tear.

Model and Methodology

For the purpose of this report, the RFR was modeled only as a structured bed. All of the important values for the parameters and equations used to calculate the parameters can be found in the Appendix of this report. The full balance equations used in the model are shown below. Note that these equations represent the 1-D model. In this report, the radial effects are not considered as they were found to have little to no effect. Initially, the temperature of the gas inside the reactor, solid, and wall were assumed to be equal to the preheating temperature of 400 °C. As The wall, solids, and internal gas temperature were constant with respect to distance

at startup [3]. Danckwerts boundary conditions were used for the inlet methane concentration and temperature of the gas when the full solution was implemented. A mathematical description of the initial and boundary conditions can be seen in the Appendix.

$$\frac{\partial y_G}{\partial t} = -\frac{u_0 \rho_{G0}}{\varepsilon_{SB} \rho_G} \frac{\partial y_G}{\partial z} + D_{eff} \frac{\partial^2 y_G}{\partial z^2} - a_G K_G (y_G - y_S) + \frac{R_{V_G}^{ho} v_G^{ho}}{C_G}$$

$$\frac{\partial T_G}{\partial t} = -\frac{u_0 \rho_{G0}}{\varepsilon_{SB} \rho_G} \frac{\partial T_G}{\partial z} + \frac{k_{G,eff}}{\rho_G Cp_G} \frac{\partial^2 T_G}{\partial z^2} - \frac{a_G h}{\rho_G Cp_G} (T_G - T_S) - \frac{4 h_{WG}}{\varepsilon_{SB} D_R \rho_G Cp_G} (T_G - T_W) + \frac{R_{V_G}^{ho} \Delta H_R}{\rho_G Cp_G}$$

$$\frac{\partial T_S}{\partial t} = \frac{k_{S,eff}}{\rho_{SB} Cp_{SB}} \frac{\partial^2 T_S}{\partial z^2} - \frac{a_S h}{\rho_{SB} Cp_{SB}} (T_S - T_G) - \frac{4 h_{WS}}{(1-\varepsilon_{SB}) D_R \rho_{SB} Cp_{SB}} (T_S - T_W) + \frac{a_S R_S^{he} \Delta H_R}{\rho_S Cp_S}$$

$$\frac{\partial T_W}{\partial t} = \frac{k_W}{\rho_W Cp_W} \frac{\partial^2 T_W}{\partial z^2} + \frac{h_{WG} D_R (T_G - T_W) + h_{WS} D_R (T_S - T_W)}{\rho_W Cp_W d_W (D_R + d_W)}$$

To solve these equations a number of initial assumptions were made. First, the feed was assumed to be an ideal gas mixture. Also, since the fraction of methane was modeled at 3,500 parts per million or less, the properties of the feed were assumed to be equal to those of air at the same temperature and pressure. Another assumption was that the pressure throughout the reactor is constant. This is validated by the work conducted by Ordonez et al. which reported a pressure drop of 0.2% for the structured bed reactor [1]. Furthermore, the heat transfer coefficient between the gas and the wall was assumed to be zero due to the fact that the gas flowing through the structured bed is not in direct contact with the reactor wall. Lastly, the homogenous reaction rate was assumed to be zero because reported that the homogenous reaction rate is only significant above temperatures of 800 °C [1]. This temperature will never be reached in the reactor as the catalyst begins to degrade at temperatures above 600 °C. This temperature then becomes the maximum temperature constraint at any point in the reactor for each cycle. Because the ignition temperature is 400 °C, as mentioned earlier, this temperature can be considered the lowest possible peak temperature in the reactor. If the maximum temperature drops below this at any point, the reaction will die out which is validated by the model [4].

A first attempt at solving the previously mentioned equations was to use MATLAB's built in PDE solver pdepe. This solver, however, was designed for parabolic type PDEs where the diffusive terms dominate. The poor performance of this tool was the first indicator that our system was dominated by convective forces, and therefore hyperbolic in nature. This is also evident by the high superficial velocity relative to reactor length and the low pressure drop. It was necessary to discretize the governing equations to produce a set of ordinary differential equations which could be solved in MATLAB. This discretization was accomplished using the method of lines technique, and originally the central finite difference method was used to evaluate the derivatives. These derivatives are shown below.

$$\frac{df}{dx} = \frac{f_{i+1} - f_{i-1}}{2h}$$

$$\frac{d^2 f}{dx^2} = \frac{f_{i+1} - 2f_i + f_{i-1}}{h^2}$$

Initial Results

Once the full model was discretized according to the finite central difference method, a series of ordinary differential equations could be solved in MATLAB for the system. To solve these equations, the MATLAB built-in ODE solver, ode15s, was used. This solver was selected due to the stiffness of the system needing to be solved. The model was carried out using 300 discretization points, and the resulting concentration and temperature profiles can be seen in Figures 1-4.

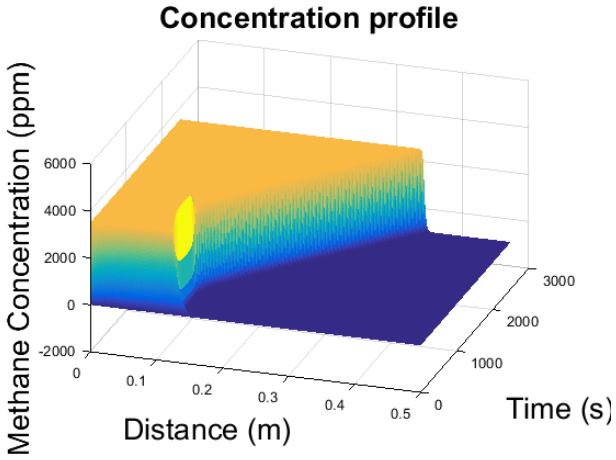

Figure 1. Concentration profile for full model and no flow reversal.

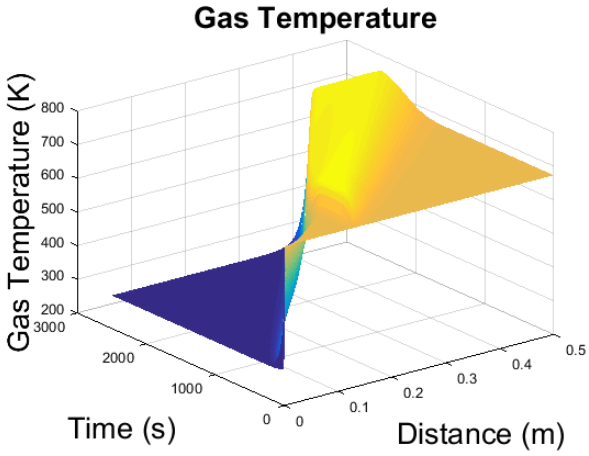

Figure 2. Gas temperature profile for full model and no flow reversal.

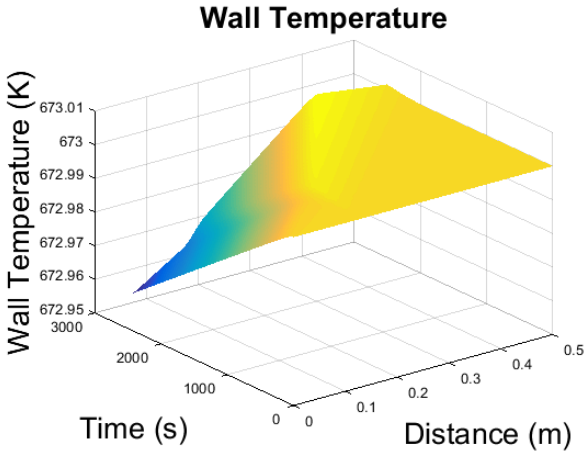

Figure 3. Wall temperature profile for full model and no flow reversal.

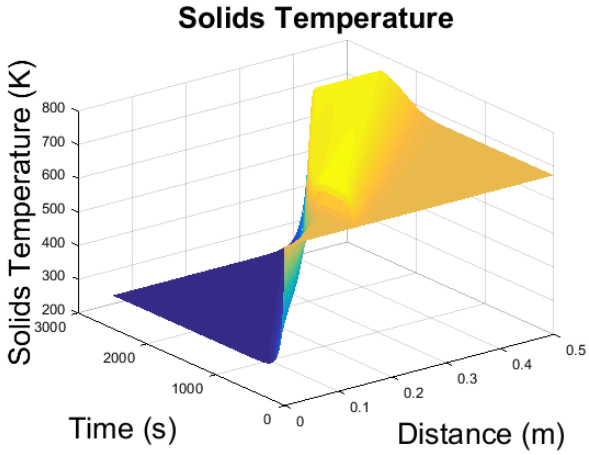

Figure 4. Solids temperature profile for full model and no flow reversal.

From these plots, it can be seen that the reaction initially occurs rapidly as the concentration of methane in the reactor quickly drops to zero upon entering the catalyst portion of the reactor.

However, as time progresses, the initial heat of the reaction is carried along the reactor and the temperature at the inlet drops due to the room temperature feed that enters. This effectively causes the concentration profile to move along the reactor as well because the reaction will not occur at temperatures below the ignition point (400 °C).

Although the results of this simulation exhibit behavior similar to those obtained by Ordonez et al., the computational time required to evaluate the model is high and the model contains moderate instability [1]. The simulation took over 600 seconds to solve the system just for one cycle with no switching (2500 seconds) on an Intel Core 2 Duo 2.67 GHz CPU processor with 3.75 GB of available memory. About half of the computational resources available were utilized and the cpu time was over 1100 seconds. Furthermore, with 300 discretization points, memory (RAM) used to store the results reached the limits of that available due to the returning of a few other metrics at each time step related to the eigenvalues of the Jacobian and its condition number. To remedy these issues, further assumptions were necessary. If fewer than 300 discretization points were used the model's stability worsened and became less physically relevant due to the presence of oscillations and overshooting. As a result of this increased stiffness the reduced strain from decreasing the number of discretization points was offset by the increased number of time steps needed to solve the system by the adaptive ode15s solver.

The first assumption that was made is that the wall is a perfect insulator [5]. The validity of this assumption is supported by the fact that the temperature profile, as shown in Figure 3, only changes by about 0.05 K and the heat transfer rate between the wall and the solids is very low. The other simplifying assumption that was made is that the diffusive effects in the reactor are negligible. This is due to the fact that the diffusive terms in the balance equations are 8 orders of magnitude less than the convective terms throughout most of the reactor. Implementing these simplifications reduces the governing equations to those shown below. In addition, the boundary conditions for the temperature of the gas and the concentration at the inlet of the reactor are now assumed to be equal to the feed temperature and concentration respectively [6].

$$\frac{\partial y_G}{\partial t} = -\frac{u_0 \rho_{G0}}{\varepsilon_{SB} \rho_G} \frac{\partial y_G}{\partial z} - a_G K_G (y_G - y_S)$$

$$\frac{\partial T_G}{\partial t} = -\frac{u_0 \rho_{G0}}{\varepsilon_{SB} \rho_G} \frac{\partial T_G}{\partial z} - \frac{a_G h}{\rho_G C p_G} (T_G - T_S)$$

$$\frac{\partial T_S}{\partial t} = -\frac{a_S h}{\rho_{SB} C p_{SB}} (T_S - T_G) + \frac{a_S R_S^{he} \Delta H_R}{\rho_S C p_S}$$

Without diffusive effects, the reaction is now entirely dependent on convection. Thus, the central finite difference method that was used previously is less suitable for the analysis of the system. Instead, the backward finite difference method is more suitable for this analysis. The first order derivatives as defined by the backward finite difference method are shown below.

$$\frac{df}{dx} = \frac{f_i - f_{i-1}}{h}$$

One other initial simplification that was attempted was to use an average temperature at each discretization point for the temperature dependent parameters included in the governing equations. However, averaging temperature resulted in nonphysical results for the concentration profile and demonstrated that the exact temperature at each point in the reactor needed to be used

to properly model the reaction. The simplification results from successfully ignoring the wall balance and diffusion effects are shown in Figures 5 and 6. The solids temperature profile is not shown as it is nearly almost identical to the gas temperature profile.

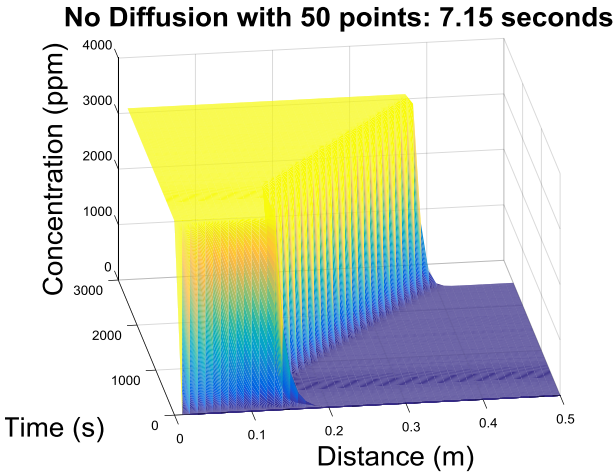

Figure 5. Concentration profile for the simplified model with no flow reversal.

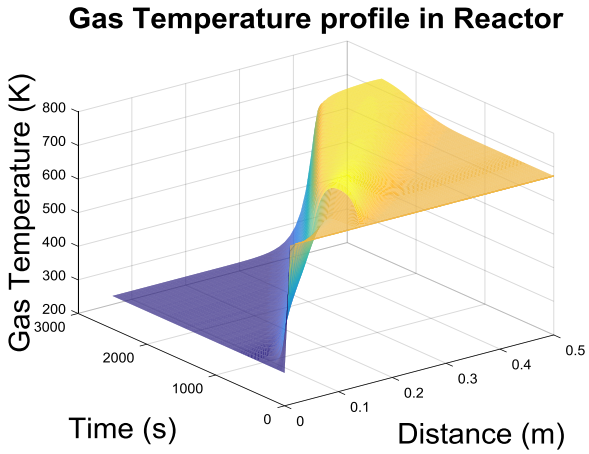

Figure 6. Gas temperature profile for the simplified model with no flow reversal.

The temperature and concentration profiles that resulted from the additional assumptions agree with those obtained from the initial model as well as those obtained by Ordonez et al [1]. Furthermore, the computational time required to evaluate the simulation of the simplified model was nearly 100 times less than the time required to evaluate the original model. The solution time was 7 seconds and the CPU time was 9 seconds. The simplified model was therefore much better for optimization and for testing sustained cycles. For example, in this model 50 cycles took roughly 250 seconds or about 4 minutes to complete as the problems stiffness reduced slightly once a pseudo-steady state was reached. To do 50 cycles with the full model would have taken over 500 minutes (almost 10 hours) and was therefore impractical.

Results after Reversing Flow

From the concentration and temperature profiles, it can be seen why switching is so necessary for this reactor to operate. Without switching, over a long enough time scale, the heat in the reactor would exit the reactor which would cause the temperature in the reactor to drop below the ignition point for the reaction [5]. This would result in zero conversion for the reactor. To prevent this, the flow is reversed, and the temperature and concentration profiles shift towards the other end of the reaction until the flow is reversed again. This can be repeated several times to achieve long term operation of the reactor [7]. To incorporate this effect into the model, the same general strategy was used. However, after a set amount of time, the calculated conditions would be reversed and the boundary conditions and initial conditions would correspond to the conditions at the end of the previous simulation [8]. The results for the model evaluated after 50 switches with the switches occurring every 2200 seconds can be seen in Figures 7-10.

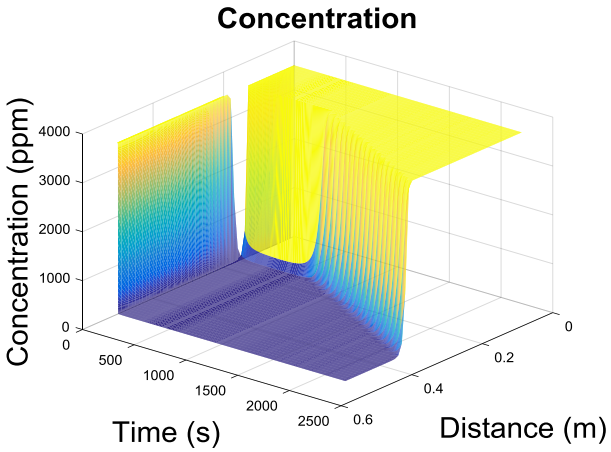

Figure 7. Concentration profile for the simplified model after 50 switches with a switching time of 2200 seconds.

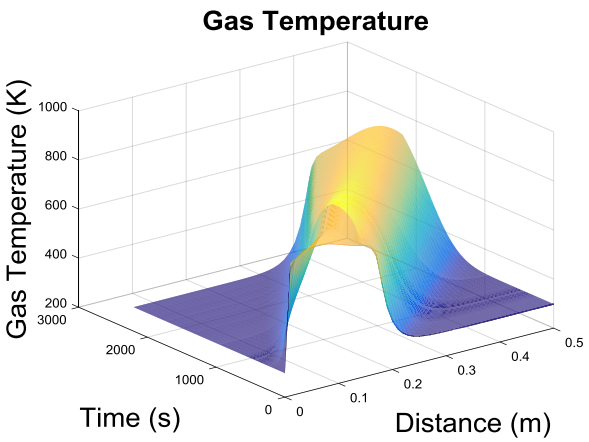

Figure 8. Gas temperature profile for the simplified model after 50 switches with a switching time of 2200 seconds.

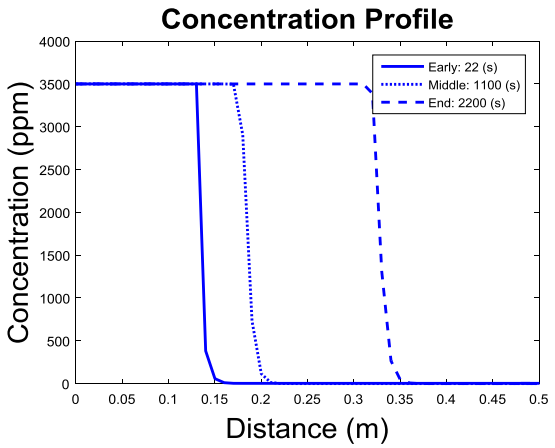

Figure 8. 2-D concentration profile for the simplified model after 50 switches with a switching time of 2200 seconds. Note that the solid line represents the early profile (22 s), the dotted line represents the middle profile (1100 s), and the dashed line represents the end profile (2200 s).

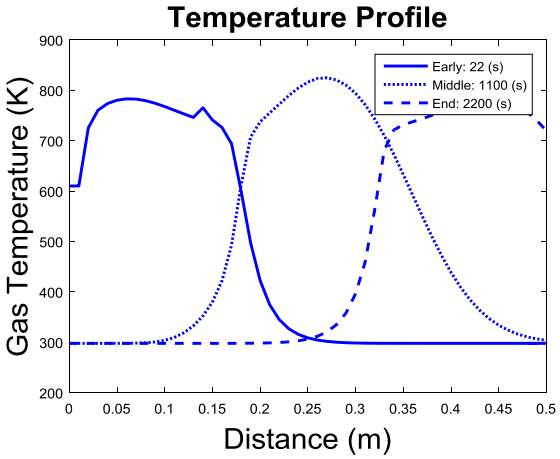

Figure 10. 2-D gas temperature profile for the simplified model after 50 switches with a switching time of 2200 seconds. Note that the solid line represents the early profile (22 s), the dotted line represents the middle profile (1100 s), and the dashed line represents the end profile (2200 s).

As shown in the figures, the heat is trapped in the reactor and continues to oscillate between the ends of the reactor even after several flow reversals. Furthermore, the reactor is able to achieve almost complete conversion of the inlet methane, although a small amount is lost after each reversal as the inlet at the instant a reversal occurs becomes the outlet and exits the reactor. Note that this pseudo steady state is reached after just a 3-4 flow reversals depending on the operating

conditions. Studies without the presence of inert showed similar concentration and temperature profiles although they were simply shifted to earlier in the reactor allowing for an increase in the minimum switching time [1].

Although there are several ways to optimize the switching time for the reactor, in this model, the switching time remained constant for each reversal and was determined by tracking how long it required for the temperature curve to move throughout the reactor. The flow was reversed when the initial increase in the temperature profile reached the end of the reactor so that the heat would not be lost. At 3500 ppm Methane and 0.1 m/s superficial velocity the switching time was found to be 2200 seconds. This time is similar to the 2000 second switching time used by Ordonez et al. In addition to determining the switching time for the specifications as outlined by Ordonez et al., the effect of different inlet conditions on switching time was evaluated as well [1]. Particularly, for an increased superficial velocity, it was found that the switching time would need to be decreased as the heat would move through the reactor at a faster rate. In addition, for a lower feed concentration, the switching time would also need to be decreased. There are two compounding reasons that decreasing the concentration makes it harder to maintain sufficient temperatures to sustain a reaction. First there is not as much heat of reaction since there is less combustible material. The other reason is that there are actually two phases in this system, a solid phase on the catalyst and a gaseous phase. The reaction only occurs in the solid phase and there is a methane concentration gradient between the catalyst solid phase and the gas phase. When the concentration of methane in the gas phase is lowered, this decreases the driving force behind the mass transfer of methane from the gas to the solid phase. For the lower inlet methane concentrations, the switching time could be kept constant if the superficial velocity was lowered as well. It was found that the reaction was sustainable for concentrations as low as 1000 ppm methane with a superficial velocity of 0.05 m/s and switching time of 2500 seconds. With some rough analysis it was found that concentrations below 700-1000 ppm could not generate enough heat to keep the temperature above the ignition point and the process would die out.

Stability Analysis

The stability of the models used in this report was analyzed through several different methods. An eigenvalue analysis was conducted on the Jacobian of the governing equations to evaluate the numerical stability of the models used. The Jacobian matrix contains all the information that determines changes in the conditions of the reactor with respect to both time and distance. Because all numerical information about the evolution of the system is in the Jacobian, it is vital that an understanding of its structure be thorough.

For the full model that included diffusion, the number of points greatly impacted the numerical stability. With less than 100 discretization points in the axial length of the reactor there were positive real eigenvalues and large imaginary parts, indicating both instability and oscillations. Both of these effects were observed when the model was run. To remove the oscillations 300 discretization steps were needed and is the same number that was used in Ordonez et al [1]. The simplified model in which diffusion was neglected was much more numerically stable, even with as few as 30 discretization steps. At no point in the simplified model were there positive real or large imaginary parts to the complex eigenvalues. The difference in numerical stability between the two models was most evident in the condition numbers of the Jacobians as the reactor progressed through time. The condition number for the full solution was on the order of 10^{11}

throughout the whole length of the reactor and the total time. This suggests that slight errors in the numbers used could lead to profound differences in the resulting time and space evolutions. For the simplified model the condition number was four orders of magnitude less. One of the more interesting observations was that the condition number tripled from the time the methane first entered the reactor, to when it first hit the discontinuity in the reactor bed as it changed from an inert material to catalyst. It is also important to note that using backwards finite differences is more stable than using the central finite differences for discretization. Because central finite differences is forward looking, large derivatives caused by steep gradients leads to oscillations as the numerical algorithm leads to a "see-saw" type effect. The plots of the full solution and simplified model condition numbers for the Jacobian for each time step can be seen in Figures 11 and 12.

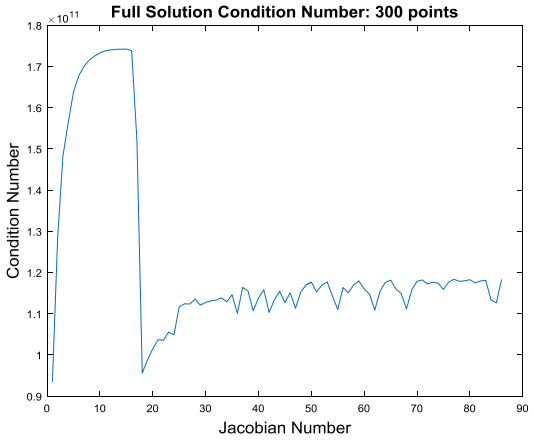

Figure 11. The condition number of the Jacobian for the full solution with 300 discretization points at each time step.

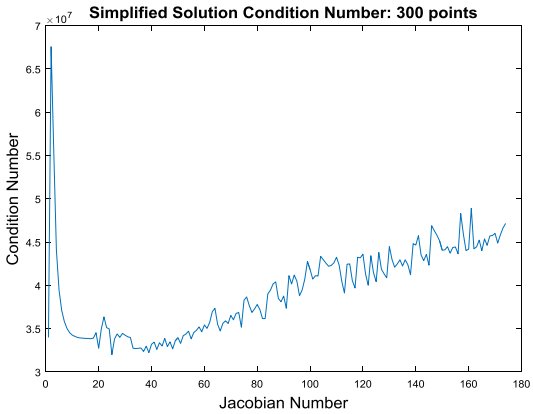

Figure 12. The condition number of the Jacobian for the simplified solution with 300 discretization points at each time step.

To test reactor stability to temporary fluctuations in the inlet methane concentration, we temporarily adjusted the boundary conditions after a few cycles had been run to reach a pseudo-steady state profile. Temporarily decreasing the concentration is not an issue as the reactor soon returns to steady state unless the dip in concentration is long enough and low enough to reduce the temperature of the reactor to below the ignition point everywhere in the reactor. Of more concern is a temporary increase that would degrade the catalyst making it inactive [3]. The effects of temporary increases are shown in Figures 13-16. Note that a reasonable increase of 1.25 times the original methane concentration of 3500 ppm for 200 seconds did not push the reactor temperature above the limiting point of 600 °C. Double the original methane concentration, however, was too much for the reactor to handle.

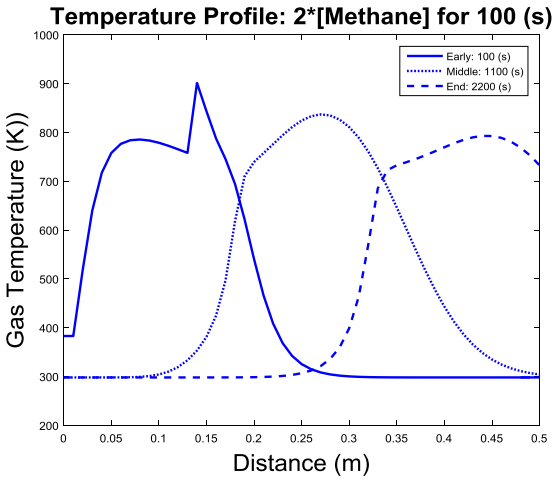

Figure 13. 2-D gas temperature profile response to an increase of 2 times the feed methane concentration. Note that the solid line represents the early profile (100 s), the dotted line represents the middle profile (1100 s), and the dashed line represents the end profile (2200 s).

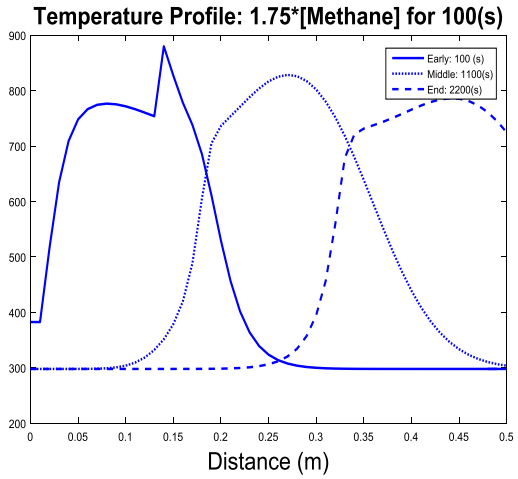

Figure 14. 2-D gas temperature profile response to an increase of 1.75 times the feed methane concentration. Note that the solid line represents the early profile (100 s), the dotted line represents the middle profile (1100 s), and the dashed line represents the end profile (2200 s).

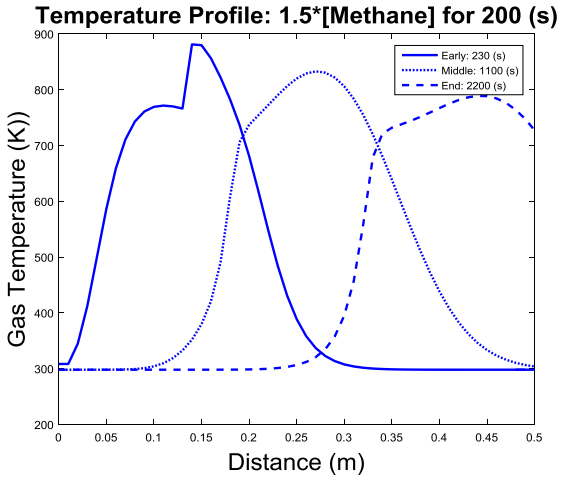

Figure 15. 2-D gas temperature profile response to an increase of 1.5 times the feed methane concentration. Note that the solid line represents the early profile (230 s), the dotted line represents the middle profile (1100 s), and the dashed line represents the end profile (2200 s).

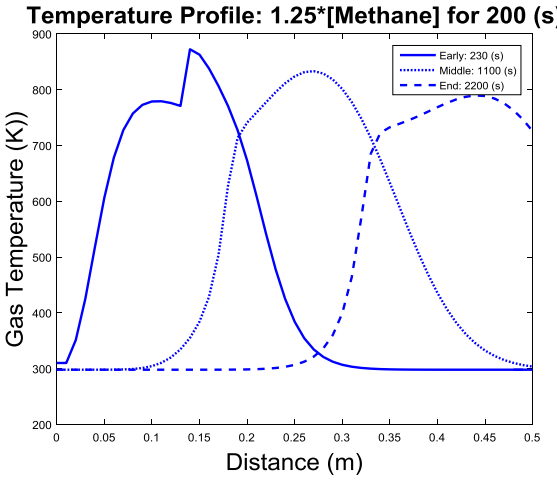

Figure 16. 2-D gas temperature profile response to an increase of 1.25 times the feed methane concentration. Note that the solid line represents the early profile (230 s), the dotted line represents the middle profile (1100 s), and the dashed line represents the end profile (2200 s).

Analysis of Inert Effects on Stability and Model Design

Inert effects were briefly mentioned previously but they will be discussed in more detail here. The reason for including inert is because, after several flow reversals, the heat gets trapped in the center of the reactor and having catalyst at the ends would be an unnecessary cost [2]. There are several effects on the actual physical process that show up and get solved for differently in the full model with diffusion and the simplified model without it.

Including the inert delays the reaction so that the concentration profile is shifted. It also provides time for the gas to heat up before hitting the catalyst portion. This means that it has a higher mass transfer rate once it hits the catalyst which leads to a slightly sharper and higher temperature peak. Because the maximum temperature is slightly higher when the inert material is included it allows sustainable cycles with lower concentrations of methane. Ordonez et al. mention that the inert can be selected for optimal heat capacity properties [1]. This means that one can select an inert to essentially preheat the feed at the inlet and act as an insulator at the exit. Literature reports also mention that inclusion of an inert causes the reactor to be more physically stable [9].

While inclusion of an inert makes the sustained reaction more stable to changes in feed concentration, it comes at a numerical price. As the flow is periodically reversed, the reaction propagates back and forth along the reactor, which creates discontinuities at the inert/catalyst boundary when solving the problem numerically. The effects in these discontinuities can be seen in the condition numbers of the Jacobian as the problem progresses through time. Once the methane gas hits the discontinuity where the inert changes to catalyst, there is a spike in the condition number as mention previously. When diffusion is included this shows up as non-real large spikes and dips in concentration above and below what is physically possible over a very short time scale. The negative dip was substantial enough in the full solution to warrant a numerical approximation for no reaction.

In the simplified model with no diffusion, the inert is modeled by setting the reaction rate equal to zero and the solid's concentration equal to the gas concentration in the ODEs that describe the first and last quarter of the reactor. This assumption is validated by the fact that there is no convective mass transfer occurring axially throughout the solid [8]. However, there is a driving force for mass transfer from point A in the gas to point A in the solid and this driving force is used to make the derivative of concentration with respect to time more negative at that point. This direct effect on the time evolution results eventually in a concentration gradient along the x-axis as well as the ODE solver finds the solution at each time step. The discontinuities in this method applied to the full solution not only created unreal spikes and dips in concentrations, but also led to increased solution time unstable solutions if too few points were used. Instead, the inert in the full solution was modeled so that the reaction rate was 10^{-15} that of the reaction rate in the catalyst.

Conclusion

Overall, we were successful in modeling the reverse flow reactor for the combustion of lean methane based on the governing mass and temperature balance equations. The results showed good agreement with the results obtained by Ordonez et al [1]. However, to obtain stable, physical results, while minimizing computational time, several simplifications were necessary.

Two significant simplifications were the assumption of the reactor wall to be a perfect insulator and neglecting the diffusive effects. The former was supported by the small temperature change along the wall when the full model was solved, and the latter was supported by the small magnitude associated with the diffusive terms. These simplifications reduced the system to a convective system that could be solved using backward finite difference method and MATLAB's built in ODE solver, ode15s. The reaction happened rapidly at first, but over time, the concentration and temperature profiles moved towards the end of the reactor. To avoid losing the heat contained in the reactor, the flow was reversed, essentially trapping the heat in the center of the reactor and enabling long term operation of the reactor. The switching time utilized in this model was 2200 seconds and was based on the rate at which the temperature profile moved along the reactor. This time agreed with the 2000 second switching time used by Ordonez et al [1]. The stability of the system was also analyzed, and it was found that the simplified model showed stability at as few as 30 discretization steps, whereas the original model required 300 discretization steps. Furthermore, it was found that the system could withstand minor step changes in inlet conditions for small amounts of time.

References

[1] Marin P., Hevia A.G., Ordonez S., and Diez F.V. "Combustion of methane lean mixtures in reverse flow reactors: Comparison between packed and structured catalyst beds." Elsevier Ltd. *Catalysis Today* **105**, 701-708 (2005).

[2] Gosiewski K., Matros Y. S., Warmuzinski K., Jaschik M., Tanczyk M. "Homogeneous vs. catalytic combustion of lean methane—air mixtures in reverse-flowreactors." *Chemical Engineering Science* **63,** 5010 – 5019 (2008).

[3] Fernandez J., Marin P., Díez F. V., Ordonez S. "Coal mine ventilation air methane combustion in a catalytic reverse flow reactor: Influence of emission humidity." *Fuel Processing Technology* **133,** 202–209 (2015).

[4] Fernandez J., Marin P., Diez F. V., Ordonez S. "Experimental demonstration and modeling of an adsorption-enhanced reverse flow reactor for the catalytic combustion of coal mine ventilation air methane*." Chemical Engineering Journal* **279**, 198–206 (2015).

[5] Munoz E., Marin P., Diez F. V., Ordonez S. "Selective catalytic reduction of NO in a reverse-flow reactor: Modelling and experimental validation." *Applied Energy* **138**, 183-192 (2015).

[6] Pawlaczyk A., Gosiewski K. "Combustion of lean methane–air mixtures in monolith beds: Kinetic studies in low and high temperatures." *Chemical Engineering Journal* **282**, 29-36 (2015).

[7] Salomons S., Hayes R. E., Poirier M., and Sapoundijiev H. "Modelling a reverse flow reactor for the catalytic combustion of fugitive methane emissions." Elsevier Ltd. Computers and Chemical Engineering 28, 1599-1610 (2004).

[8] Zhang J., Lei Z., Li J., Chen B. "Simulation of a Reverse FlowReactor for the Catalytic Combustion of Lean Methane Emissions." *Chinese Journal of Chemical Engineering* **22**, 843-853 (2014).

[9] Zhu Y., Chen G., Li X., Yang G. "Resonance Response of Reverse Flow Reactors: A Numerical Simulation." *Ind. Eng. Chem. Res.* **54**, 5885-5893 (2015).

Appendix

Governing Equations:

$$\frac{\partial y_G}{\partial t} = -\frac{u_0 \rho_{G0}}{\varepsilon_{SB} \rho_G}\frac{\partial y_G}{\partial z} + D_{eff}\frac{\partial^2 y_G}{\partial z^2} - a_G K_G (y_G - y_S) + \frac{R_{V_G}^{ho} v_G^{ho}}{C_G} \tag{1-3}$$

$$\frac{\partial T_G}{\partial t} = -\frac{u_0 \rho_{G0}}{\varepsilon_{SB} \rho_G}\frac{\partial T_G}{\partial z} + \frac{k_{G,eff}}{\rho_G Cp_G}\frac{\partial^2 T_G}{\partial z^2} - \frac{a_G h}{\rho_G Cp_G}(T_G - T_S) - \frac{4h_{WG}}{\varepsilon_{SB} D_R \rho_G Cp_G}(T_G - T_W) + \frac{R_{V_G}^{ho} \Delta H_R}{\rho_G Cp_G} \tag{2-3}$$

$$\frac{\partial T_S}{\partial t} = \frac{k_{S,eff}}{\rho_{SB} Cp_{SB}}\frac{\partial^2 T_S}{\partial z^2} - \frac{a_S h}{\rho_{SB} Cp_{SB}}(T_S - T_G) - \frac{4h_{WS}}{(1-\varepsilon_{SB}) D_R \rho_{SB} Cp_{SB}}(T_S - T_W) + \frac{a_S R_S^{he} \Delta H_R}{\rho_S Cp_S} \tag{3-3}$$

$$\frac{\partial T_W}{\partial t} = \frac{k_W}{\rho_W Cp_W}\frac{\partial^2 T_W}{\partial z^2} + \frac{h_{WG} D_R (T_G - T_W) + h_{WS} D_R (T_S - T_W)}{\rho_W Cp_W d_W (D_R + d_W)} \tag{4-3}$$

Boundary Conditions:

$$y_G(0,t) = y_{G0} + \frac{\varepsilon_{SB} D_{eff}}{u_0}\left(\frac{\partial y_G}{\partial z}\right)_{z=0} \tag{5-3}$$

$$T_G(0,t) = T_{G0} + \frac{\varepsilon_{SB} k_{G,eff}}{u_0 \rho_{G0} Cp_G}\left(\frac{\partial T_G}{\partial z}\right)_{z=0} \tag{6-3}$$

$$\left(\frac{\partial T_S}{\partial z}\right)_{z=0} = 0 \tag{7-3}$$

$$\left(\frac{\partial T_W}{\partial z}\right)_{z=0} = 0 \tag{8-3}$$

$$\left(\frac{\partial y_G}{\partial z}\right)_{z=L_R} = 0 \tag{9-3}$$

$$\left(\frac{\partial T_G}{\partial z}\right)_{z=L_R} = 0 \tag{10-3}$$

$$\left(\frac{\partial T_S}{\partial z}\right)_{z=L_R} = 0 \tag{11-3}$$

$$\left(\frac{\partial T_W}{\partial z}\right)_{z=L_R} = 0 \tag{12-3}$$

Initial Conditions:

$$y_G(z,0) = 0 \tag{13-3}$$

$$T_G(z,0) = T_{Pre} \tag{14-3}$$

$$T_S(z,0) = T_{Pre} \tag{15-3}$$

$$T_W(z,0) = T_{Pre} \tag{16-3}$$

Miscellaneous Parameters:

$$\rho_G = 28.97 \times 10^{-3} \times \frac{P_0}{RT_G} \quad (14\text{-}3)$$

$$D_{AB} = 9.86 \times 10^{-10} \times T_G(z,t)^{1.75} \quad (15\text{-}6)$$

$$D_{eff} = D_{AB} + \frac{(vD_H)^2}{196D_{AB}} \quad (16\text{-}6)$$

$$\mu = 7.701 \times 10^{-6} + 4.166 \times 10^{-8} T_G(z,t) - 7.531 \times 10^{-12} T_G(z,t)^2 \quad (17\text{-}6)$$

$$Re = \frac{u_0 D_H \rho_G}{\mu} \quad (18\text{-}6)$$

$$Sc = \frac{u_0}{\rho_G \mu} \quad (19\text{-}6)$$

$$Sh = \frac{K_G D_H}{D_{AB}} = 2 + 1.1 Sc^{1/3} Re^{0.6} \quad (20\text{-}6)$$

$$k_{VC} = A^{he} \exp\left(-\frac{Ea}{RT_S(z,t)}\right) \quad (21\text{-}3)$$

$$D_K = 97 \frac{d_{pores}}{2} \left(\frac{T_S(z,t)}{M}\right)^{0.5} \quad (22\text{-}6)$$

$$D_{eff,p} = \frac{D_K \varepsilon_{pores}}{\tau_{pores}} \quad (23\text{-}6)$$

$$\phi = L_C \left(\frac{k_{VC}}{D_{eff,p}}\right)^{0.5} \quad (24\text{-}3)$$

$$\eta = \frac{\tanh(\phi)}{\phi} \quad (25\text{-}3)$$

$$k_S^{he} = L_C k_{VC} \quad (26\text{-}3)$$

$$y_S = \frac{y_G(z,t)}{\left(1 + \left(\frac{\eta k_S^{he}}{K_G}\right)\right)} \quad (27\text{-}3)$$

$$Pe = \frac{u_0 D_H \rho_G Cp_G}{k_{G,eff}} = \left(\frac{0.73\varepsilon}{ReSc} + \frac{0.5}{1 + \frac{9.7\varepsilon}{ReSc}}\right)^{-1} \quad (28\text{-}6)$$

$$k_G = 0.01679 + 5.073 \times 10^{-5} \times T_G(z,t) \quad (29\text{-}6)$$

$$Pr = \frac{Cp_G \mu}{k_G} \quad (30\text{-}6)$$

$$Gz = \frac{D_H}{0.5RePr} \quad (31\text{-}6)$$

$$Nu_T = \frac{hD_H}{k_G} = 2.977 \left(1 + 3.6 Gz^{0.5} \exp\left(-\frac{50}{Gz}\right)\right) \quad (32\text{-}6)$$

$$k_{S,eff} = k_{SB}(1 - \varepsilon_{SB}) \quad (33\text{-}3)$$

$$a_S = \frac{a_G \varepsilon_{SB}}{1 - \varepsilon_{SB}} \quad (34\text{-}3)$$

$$C_G = \frac{P_0}{RT_G(z,t)} \quad (35\text{-}3)$$

$$R_S^{he} = -\frac{\eta k_S^{he} C_G y_S}{10^{-6}} \quad (36\text{-}3)$$

Note that the equations are numbered (#-i) where i represents which reference paper the equations were obtained from.

Variable	Parameter	Value	Units
a_G	Surface – volume ratio for gas phase	3448	m^{-1}
a_S	Surface – volume ratio for solid phase	6694	m^{-1}
A^{he}	Heterogeneous reaction pre-exponential factor	1.58×10^{-11}	m^3/s-m^3 cat
C_G	Molar concentration in the gas phase		mol/m^3
Cp_G	Gas phase heat capacity	10^{-3}	J/kg-K
Cp_{SB}	Structured bed heat capacity	965	J/kg-K
Cp_W	Wall heat capacity	500	J/kg-K
d_{pores}	Mean catalyst pore diameter	6.377×10^{-9}	m
D_{AB}	Methane – air molecular diffusion coefficient		m^2/s
D_{eff}	Axial mass dispersion coefficient		m^2/s
$D_{eff,p}$	Pore effective diffusivity		m^2/s
D_H	Structured bed hydraulic diameter	0.0116	m
D_K	Knudsen diffusion coefficient		m^2/s
D_R	Reactor internal diameter	0.05	m
Ea	Heterogeneous reaction activation energy	112,500	J/mol
Gz	Graetz number		
h	Gas – solid heat transfer coefficient		W/m^2-K
h_{WS}	Wall – solid heat transfer coefficient	0.00021	W/m^2-K
k_G	Thermal conductivity of the gas phase		W/m-K
$k_{G,eff}$	Effective thermal conductivity of the gas phase		W/m-K
k_{SB}	Thermal conductivity of the structured bed	2.15	W/m-K
$k_{S,eff}$	Effective thermal conductivity of the solid phase	0.731	W/m-K
k_S^{he}	Heterogeneous kinetic constant per catalyst surface		m^3/s-m^3 cat
k_{VC}	Kinetic constant per catalyst volume		m^3/s-m^3 cat
k_W	Thermal conductivity of the wall	19.51	W/m-K
K_G	Gas – solid mass transfer coefficient		m/s
L_C	Effectiveness washcoat thickness	0.000046	m
L_R	Reactor length	0.5	m
M	Gas molar mass	0.028	kg/mol
N_m	Cell Density	400	cpsi
Nu_T	Structured bed Nusselt number		
P_0	Pressure	120,000	Pa
Pe	Peclet number		
Pr	Prandtl number		
R	Ideal gas constant	8.314	J/mol-K
Re	Reynolds number		
R_S^{he}	Heterogeneous reaction rate per catalyst surface		mol/m^2-s

Table 1. Descriptions and values when possible for variables used in the equations.[3,6]

Variable	Parameter	Value	Units
Sc	Schmidt number		
Sh	Sherwood number		
t	Time		s
T_G	Temperature of the gas phase		K
T_{G0}	Feed temperature of the gas phase	298	K
T_{Pre}	Preheating temperature	673	K
T_S	Temperature of the solid phase		K
T_W	Temperature of the wall		K
u_0	Surface velocity	0.1	m/s
v	Interstitial velocity	0.066	m/s
y_G	Methane mole fraction in gas phase		ppmV
y_{G0}	Methane mole fraction in reactor feed	3500	ppmV
y_S	Methane mole fraction in solid phase		ppmV
z	Axial position along reactor		m
ΔH_R	Enthalpy of reaction	-802,500	J/mol
ε_{pores}	Pore void fraction	0.519	
ε_{SB}	Structured bed void fraction	0.66	
η	Internal effectiveness		
μ	Gas viscosity		Pa-s
ρ_G	Density of gas phase		kg/m^3
ρ_{G0}	Density of gas phase at start	1.4	kg/m^3
ρ_{SB}	Density of the structured bed	2500	kg/m^3
ρ_W	Density of the wall	7700	kg/m^3
τ_{pores}	Pore tortuosity	2	
ϕ	Thiele modulus		

Table 1. Descriptions and values when possible for variables used in the equations.[3,6]